

# Probing the ultrafast gain and refractive index dynamics of a VECSEL

Cite as: Appl. Phys. Lett. **119**, 191105 (2021); <https://doi.org/10.1063/5.0061346>

Submitted: 25 June 2021 • Accepted: 25 October 2021 • Published Online: 09 November 2021

 C. Kriso,  T. Bergmeier,  N. Giannini, et al.



View Online



Export Citation



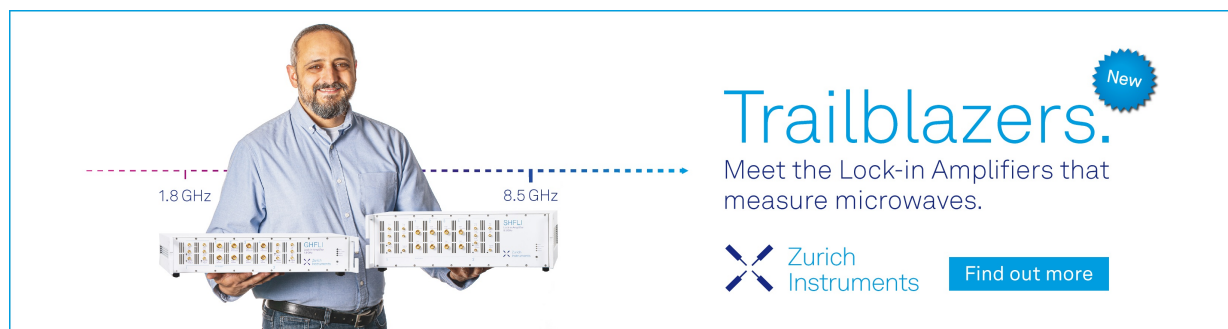
CrossMark

## ARTICLES YOU MAY BE INTERESTED IN

[High-power operations of single-mode surface grating long oxide aperture VCSELs](#)  
Applied Physics Letters **119**, 191103 (2021); <https://doi.org/10.1063/5.0066590>

[Opportunities for hybrid diamond nanosensors targeting photothermal applications in biological systems](#)  
Applied Physics Letters **119**, 190502 (2021); <https://doi.org/10.1063/5.0063089>

[Temperature-sensitive mechanism for silicon blocked-impurity-band photodetectors](#)  
Applied Physics Letters **119**, 191104 (2021); <https://doi.org/10.1063/5.0065468>



**Trailblazers.** 

Meet the Lock-in Amplifiers that measure microwaves.

 Zurich Instruments [Find out more](#)

# Probing the ultrafast gain and refractive index dynamics of a VECSEL

Cite as: Appl. Phys. Lett. **119**, 191105 (2021); doi: [10.1063/5.0061346](https://doi.org/10.1063/5.0061346)

Submitted: 25 June 2021 · Accepted: 25 October 2021 ·

Published Online: 9 November 2021



View Online



Export Citation



CrossMark

C. Kriso,<sup>1,a)</sup> T. Bergmeier,<sup>1</sup> N. Giannini,<sup>2</sup> A. R. Albrecht,<sup>2</sup> M. Sheik-Bahae,<sup>2</sup> S. Benis,<sup>3</sup> S. Faryadras,<sup>3</sup> E. W. Van Stryland,<sup>3</sup> D. J. Hagan,<sup>3</sup> M. Koch,<sup>1</sup> G. Mette,<sup>1</sup> and A. Rahimi-Iman,<sup>1,a)</sup>

## AFFILIATIONS

<sup>1</sup>Department of Physics and Material Sciences Center, Philipps-Universität Marburg, Renthof 5, 35032 Marburg, Germany

<sup>2</sup>Department of Physics and Astronomy, University of New Mexico, 210 Yale Blvd. NE, Albuquerque, New Mexico 87131, USA

<sup>3</sup>CREOL, The College of Optics and Photonics, University of Central Florida, Orlando, Florida 32816, USA

<sup>a)</sup>Authors to whom correspondence should be addressed: [christian.kriso@physik.uni-marburg.de](mailto:christian.kriso@physik.uni-marburg.de) and [a.r-i@physik.uni-marburg.de](mailto:a.r-i@physik.uni-marburg.de)

## ABSTRACT

Typically, strong gain saturation and gain dynamics play a crucial role in semiconductor laser mode-locking. While there have been several investigations of the ultrafast gain dynamics in vertical-external-cavity surface-emitting lasers (VECSELs), little is known about the associated refractive index changes. Yet, such refractive index changes do not only have a profound impact on the pulse formation process leading to self-phase modulation, which needs to be compensated by dispersion, but they are also of particular relevance for assessing the feasibility of Kerr-lens mode-locking of VECSELs. Here, we measure both refractive index as well as gain dynamics of a VECSEL chip using the ultrafast beam deflection method. We find that, in contrast to the gain dynamics, the refractive index dynamics is dominated by an instantaneous ( $\sim 100$  fs) and a very slow component ( $\sim 100$  ps). The time-resolved measurement of nonlinear refraction allows us to predict a pulse-length dependent, effective nonlinear refractive index  $n_{2,eff}$ , which is shown to be negative and on the order of  $10^{-16}$  m<sup>2</sup>/W for short pulse lengths ( $\sim 100$  fs). It becomes positive for large excitation fluences and large pulse lengths (few ps). These results agree with some previous reports of self-mode-locked VECSELs for which the cavity design and pulse properties determine sign and strength of the nonlinear refractive index when assuming Kerr-lens mode-locking.

Published under an exclusive license by AIP Publishing. <https://doi.org/10.1063/5.0061346>

Ultrashort-pulse mode-locking and frequency combs have emerged as a major topic in semiconductor laser research, and state-of-the-art semiconductor disk laser systems (or VECSELs) are under development that utilize passive mode-locking with various applications in mind such as spectroscopy, biomedicine, and nonlinear optics.<sup>1–3</sup> Mostly optically pumped, VECSELs combine flexible wavelength design of the gain chip, high optical output powers, and excellent beam quality.<sup>4–6</sup> The external cavity allows us to further functionalize the laser emission, for example, to achieve single-frequency generation or nonlinear frequency conversion by inserting optical filters or nonlinear crystals into the cavity, respectively.<sup>7,8</sup>

Mode-locking can routinely be achieved by inserting semiconductor-saturable absorber mirrors (SESAMs) into the cavity with the possibility of obtaining ultrashort pulses in the sub-100 fs regime as well as peak powers of several kilowatts.<sup>9–11</sup>

In this context, recently also saturable-absorber-free mode-locking, usually referred to as “self-mode-locking,” has received considerable attention and has been demonstrated by several groups.<sup>12–16</sup>

These results remain subject of ongoing debate within the community concerning what the driving mechanisms behind this phenomenon are, and whether those truly lead to a mode-locked state of the laser.<sup>17–19</sup> Both, mode-locking by a four-wave-mixing nonlinearity in the gain chip<sup>19</sup> and Kerr-lens mode-locking have been discussed as possible explanations.<sup>14</sup> In particular, the latter hypothesis triggered considerable efforts to characterize the nonlinear refractive index of the gain chip under realistic conditions, i.e., using probe irradiances and excitation fluences comparable to how they occur in a mode-locked VECSEL.<sup>20–24</sup> However, most of these investigations have been performed using pulse lengths of only a few hundreds of femtoseconds. Yet, pulses generated by self-mode-locked VECSELs usually are longer, that is, in the few-ps regime down to sub-ps pulse durations.<sup>18</sup> Therefore, considering the strong gain dynamics of semiconductor lasers, which intrinsically affects the refractive index of the gain chip, such nonlinear lensing investigations so far have not provided a very accurate picture of the nonlinear refractive index of the gain chip. Time-resolved measurements of the refractive index dynamics of a

VECSEL would, therefore, allow us to obtain a more realistic estimate of the strength of nonlinear lensing in VECSELs. Beyond this, it would allow us to obtain insight into the phase dynamics that affects a short pulse in VECSEL mode-locking. In phenomenological modeling of pulse formation, this is usually taken into account by introducing a constant, the linewidth enhancement factor, which relates gain changes to phase changes.<sup>25,26</sup> However, this is a strongly simplifying assumption, and therefore, the full knowledge of the refractive index dynamics might improve modeling significantly.

In this work, we measure the time-resolved nonlinear optical response of a gain chip using the recently developed ultrafast beam-deflection technique.<sup>27</sup> This uniquely enables us to simultaneously acquire gain as well as refractive index dynamics. Moreover, we validate the results by additional Z-scan measurements well known from effective nonlinear lensing characterization of materials without temporal resolution.<sup>28</sup>

Our pump-probe setup, including a prepulse for excitation of the sample, is displayed in Fig. 1(a). Here, the probe spot is overlapped with the pump spot on the sample in a way that it sits exactly on the position of the largest slope of the Gaussian-shaped intensity profile of the pump as shown in Fig. 1(b) (which requires that the probe spot diameter is considerably smaller than the pump at the position of the sample). Consequently, the refractive index changes induced by the pump in the sample will lead to a deflection of the probe, which is proportional to the refractive index change of the sample and can be detected by a segmented photodetector. In our scheme, we use lock-in detection to measure both pump-induced transmission changes by recording the sum signal of the segmented detector and pump-induced deflection changes by recording the difference signal of the

segmented detector. When varying the delay between the pump and probe pulse, we can record time-resolved changes of transmission and deflection. For the beam deflection measurements, we used a 200 kHz femtosecond laser system (Light Conversion Carbide) pumping two optical parametric amplifiers (OPAs). With one OPA (Orpheus-F), we generated pulses at a center wavelength of 1163 nm and, with another OPA (Orpheus-N-2H), pulses at a center wavelength of 780 nm. The latter is used to excite the sample with a prepulse arriving at the sample about 100 ps before the pump-probe measurement takes place. For the pump-probe measurements, a filter with a center wavelength of 1150 nm and a bandwidth of 25 nm was used to align the laser spectrum with respect to the photoluminescence of the VECSEL sample (shown in the [supplementary material](#)). The pump and probe beams are obtained by splitting the 1150 nm laser beam with a 90:10-beam splitter. A half-wave plate and calcite polarizers are used to ensure good orthogonal polarization of the pump and the probe with respect to each other. The probe beam is attenuated by neutral-density filters in order to prevent detector saturation. To block the pump from reaching the detector, an iris and a polarizer are used, which only transmit the probe. The half width (HW)  $1/e^2$  of the probe beam at its focus and of the pump spot at the same position are 29 and 97  $\mu\text{m}$ , respectively. Both, the pump-induced transmission and deflection signal scale approximately linearly when increasing the pump irradiance, as verified with reference samples (see the [supplementary material](#)). The spot size of the excitation is made a lot larger (with a HW  $1/e^2$  of about 500  $\mu\text{m}$  on the chip) to ensure an approximately homogeneous sample excitation at the area where the pump-probe measurement takes place. A long-pass filter is inserted after the sample to prevent the excitation beam at 780 nm from scattering into the detector.

The VECSEL sample used in this investigation consists of a resonant periodic gain structure of 10 InGaAs quantum wells separated by GaAsP barriers for strain compensation and was grown by metalorganic chemical vapor deposition (MOCVD). Two InGaP layers of approximately 190 nm thickness surround the structure for charge carrier confinement. The sample used here is a distributed Bragg reflector (DBR)-free VECSEL or a membrane external-cavity surface emitting laser (MECSEL). The GaAs growth substrate is etched away, and the structure is van-der-Waals-bonded onto a 350  $\mu\text{m}$  thick 4H-SiC heat spreader. MECSELs have been shown to exhibit an extraordinarily large wavelength tuning range and excellent thermal properties.<sup>29–31</sup> In this work, it enables us to conduct the beam deflection measurements in transmission geometry rather than in reflection, which greatly simplifies the experiment.

In the following, we investigate beam deflection measurements for different excitation fluences ranging from 1.1 to 21.2  $\mu\text{J}$  and a fixed pump peak irradiance (1 GW/cm<sup>2</sup>). Figures 2(a) and 2(b) show the normalized pump-induced transmission changes  $\Delta T/T$  and the deflection changes  $\Delta E/E$  as a function of the delay between the pump and the probe pulse, respectively. Transmission changes  $\Delta T$  are normalized with respect to the total signal of the probe in the absence of the pump,  $T$ , and deflection changes  $\Delta E$  are normalized with respect to  $E = T + \Delta T$ , which also takes into account the transmission changes of the probe during the deflection measurement.

When the sample is only weakly excited, the probe pulse experiences first an increase in transmission before decaying back to a transmission change of close to zero. The deflection signal experiences a very fast negative response and subsequently a rather constant

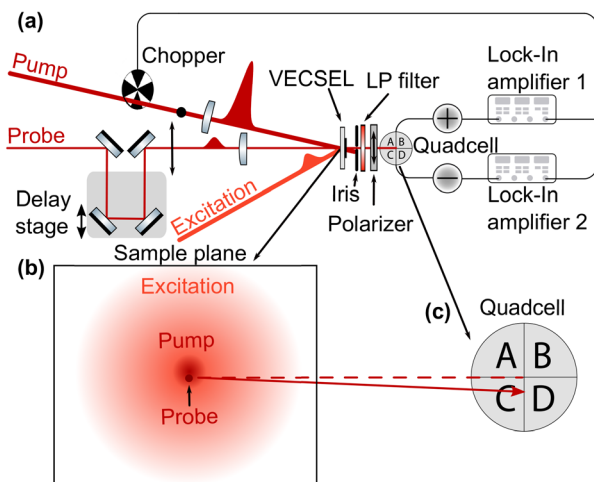


**FIG. 1.** (a) Beam-deflection setup for measuring time-resolved transmission and refractive index changes of the VECSEL. A prepulse (at 780 nm), arriving 100 ps before the pump-probe measurement (at 1150 nm) takes place, excites the sample. Two lock-in amplifiers are used to measure simultaneously the sum (“+”) and difference (“−”) signal of the segmented detector (“Quadcell”). (b) View on the sample (VECSEL) surface displaying the approximate size ratio and the relative position of the spots of excitation as well as the pump and the probe beam. (c) The pump-induced refractive index change in the sample will lead to a deflection of the probe beam that will be detected by a non-zero difference signal between the upper and lower half of the segmented detector.

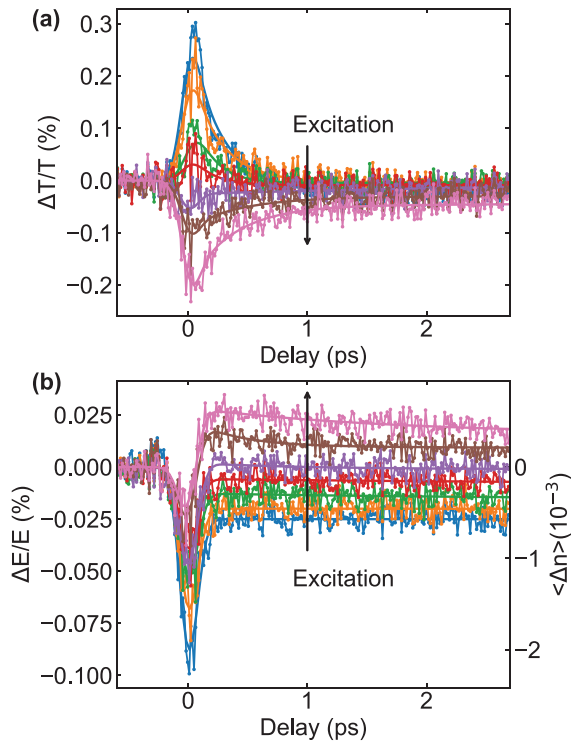


**FIG. 2.** (a) Normalized probe transmission and (b) deflection of VECSELs for a pump irradiance of  $1 \text{ GW/cm}^2$  and various excitation fluences (1.1, 2.8, 6.0, 8.7, 10.2, 13.0, and  $21.2 \mu\text{J/cm}^2$  in the direction of the arrow). The probe beam experiences increased transmission when the pump experiences absorption and opposite behavior in the case of gain. The solid line displays the model used to fit the data [Eq. (2)]. The right axis in (b) displays the refractive index change averaged over the width of the cross correlation of the pump and the probe pulse ( $\sim 180$  fs FWHM) that corresponds to the measured deflection.

negative deflection signal over the few-ps timescale. Negative deflection corresponds to a negative refractive index change.

When the sample is strongly excited, the probe experiences first a strong decrease in transmission and subsequently a recovery to a slightly negative transmission change. This offset from zero transmission change at longer times indicates that the pump beam experiences net gain. Note that the probe beam will experience increased absorption when the pump experiences gain and opposite behavior in the case of absorption.<sup>32</sup> This behavior is due to the saturation of absorption and gain by the high-fluence pump pulse and its subsequent recovery due to the various processes described in the next paragraph.<sup>33</sup> The deflection signal becomes positive for long time scales and large excitation fluences.

Both, transmission and deflection measurements can be modeled by a response function of the form

$$R(t) = \left( b_0 e^{-\frac{t}{\tau_0}} + b_1 e^{-\frac{t}{\tau_1}} \right) \theta(t) + b_2 \delta(t), \quad (1)$$

where  $\theta(t)$  and  $\delta(t)$  are the Heaviside and Dirac delta functions, respectively. The time constant  $\tau_0$  models the non-instantaneous response of the sample consisting of carrier cooling in the absorption regime and carrier heating in the gain regime, which occur with a time

constant of several hundreds of fs. The time constant  $\tau_1$  is usually in the order of magnitude of hundreds of ps or few ns and describes carrier relaxation or refilling.<sup>34</sup> The instantaneous response described by the Dirac delta function models both contributions from two-photon absorption or the ultrafast Kerr effect as well as relaxation of the excited carriers into a Fermi–Dirac distribution in the absorption regime or filling of the spectral holes in the gain regime, which is too fast to be resolved by the measurement conducted with a pump and a probe pulse with a full-width at half maximum (FWHM) of 130 fs, respectively.

This response function is fitted to the experimental traces by

$$\frac{\int_{-\infty}^{+\infty} \int_{-\infty}^{+\infty} R(t-t') I_{pu}(t') dt' I_{pr}(t-\tau) dt}{\int_{-\infty}^{+\infty} I_{pr}(t) dt}. \quad (2)$$

Here,  $I_{pu}$  and  $I_{pr}$  represent the intensity envelope of the pump and the probe pulse, respectively.

When fitting the pump-probe measurement of the transmission changes with Eqs. (1) and (2), one obtains a time constant  $\tau_0$  of 300–400 fs for carrier cooling, i.e., when the sample is in the absorption regime and only weakly excited. This corresponds to values measured in Ref. 35. When the sample is strongly excited, this time constant increases slightly to 400–500 fs, corresponding to the time the carrier-distribution heats up to the lattice temperature. In comparison to the measurement of Ref. 36, the ultrafast gain recovery also contains a pronounced instantaneous component ( $\sim 100$  fs) for large excitation fluences.

Interestingly, the effect of carrier cooling/heating, i.e., the component with a sub-ps time constant, is not very strong in the measurement of the deflection signal [Fig. 2(b)], as that signal mostly consists of an ultrafast ( $\sim 100$  fs) and a very slow component ( $\sim 100$  ps). In contrast to measurements of semiconductor optical amplifiers, the instantaneous negative decrease in the refractive index reduces significantly with increased excitation fluence, while otherwise the trend is similar.<sup>32,37</sup>

The time-resolved deflection measurement can be mapped to the refractive index change averaged over the length of the probe pulse,  $\langle \Delta n(\tau) \rangle$ , where  $\tau$  represents the delay between the pump and probe pulse. This is done by comparing the deflection signal of the VECSEL to the deflection signal of a reference sample (SiC) with a known nonlinear refractive index  $n_2$  (see the [supplementary material](#) for more details of this procedure). The right axis of Fig. 2(b) displays the corresponding  $\langle \Delta n(\tau) \rangle$  for the measurement of the VECSEL sample.

The response function, obtained by fitting  $\langle n(\tau) \rangle$  to Eq. (2), can be used to calculate the effective nonlinear refractive index  $n_{2,eff}$ . This quantity describes the nonlinear refractive index that would be seen by a single beam propagating through the sample, for example, when performing a Z-scan measurement, and depends on the pulse length. It relates to the total refractive index change by  $\Delta n = n_{2,eff} I$ , with  $I$  being the irradiance of the single beam. It can be calculated by<sup>38</sup>

$$n_{2,eff} = \frac{\int_{-\infty}^{+\infty} \int_{-\infty}^{+\infty} R(t-t') I(t') dt' I(t) dt}{\int_{-\infty}^{+\infty} I^2(t) dt}. \quad (3)$$

Here,  $I(t)$  is the intensity pulse envelope of the single beam. Figure 3(a) shows the excitation-dependent  $n_{2,eff}$  calculated from various

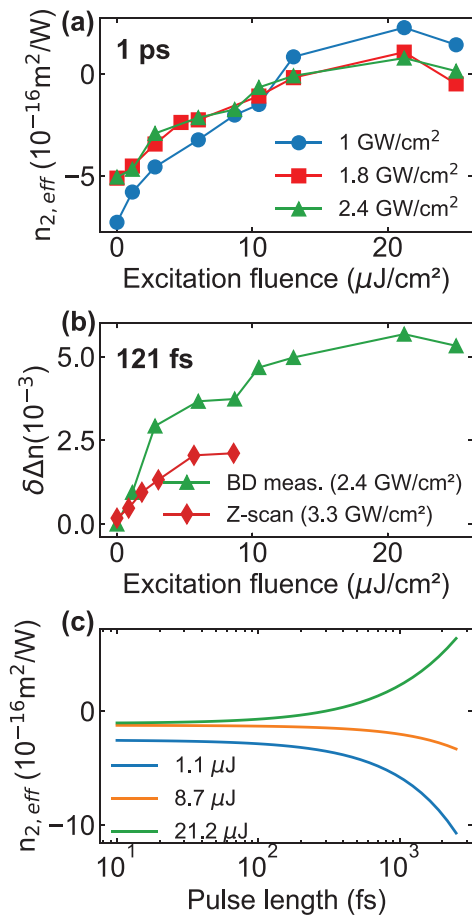


**FIG. 3.** (a) Effective, excitation-dependent, nonlinear refractive index  $n_{2,eff}$  calculated for a pulse length (FWHM) of 1 ps and several pump peak irradiances. (b) Excitation-induced refractive index change  $\delta\Delta n$  obtained from a Z-scan measurement conducted with a peak irradiance of  $3.3 \text{ GW/cm}^2$  and a pulse length (FWHM) of 121 fs and the beam deflection measurement performed with  $2.4 \text{ GW/cm}^2$  pump peak irradiance. (c) Calculated  $n_{2,eff}$  as a function of the pulse length (FWHM) for different excitation fluences and a pump peak irradiance of  $1 \text{ GW/cm}^2$ . The calculation of  $n_{2,eff}$  [Eq. (3)] is based on the fitted response function of the nonlinear refractive index change.

deflection measurements with different pump irradiances for a pulse length of 1 ps. One can see that  $n_{2,eff}$  is similar for all pump irradiances, being around  $-6 \times 10^{-16} \text{ m}^2/\text{W}$  for no excitation and increasing to slightly positive values of around  $+2 \times 10^{-16} \text{ m}^2/\text{W}$  for large excitation fluences. The fact that  $n_{2,eff}$ , calculated for 1 ps, is approximately independent of the pump irradiance demonstrates the third-order character of the nonlinearity for both the instantaneous ( $\sim 100$  fs) and the slower component ( $\sim 1$  ps).

In addition to the beam deflection measurements, Z-scan measurements were performed on the unexcited sample, which yield an  $n_{2,eff}$  of  $-1.2 \times 10^{-16} \text{ m}^2/\text{W}$ . This corresponds in sign and order of magnitude to the  $n_{2,eff}$  of around  $-3 \times 10^{-16} \text{ m}^2/\text{W}$  calculated from the beam deflection measurements with the Z-scan pulse length of 121 fs. Furthermore, the trend of the refractive index change with increasing excitation was measured by Z-scan and is compared in Fig. 3(b) to

the beam deflection measurement with relatively good agreement of both measurements. For details of the measurement of the excitation-induced refractive index change  $\delta\Delta n$ , we refer to the [supplementary material](#). Also, we note that both the order of magnitude of  $n_{2,eff}$  and the trend with increasing excitation correspond to previous measurements of nonlinear refraction in VECSELS as well as theoretical investigations.<sup>21–24,39</sup>

We proceed to calculate the pulse-length dependent  $n_{2,eff}$  for several excitation fluences as shown in Fig. 3(c). It can be seen that, for low excitation fluences,  $n_{2,eff}$  is negative for all pulse lengths and increases strongly in magnitude for pulse lengths larger than 1 ps. This is a consequence of the nearly constant refractive index change at longer delays as shown in Fig. 2(b). In contrast, for large excitation fluences,  $n_{2,eff}$  changes sign from negative to positive when going to pulse lengths beyond 1 ps.

It is interesting to compare the trend of the pulse width-dependent, as well as the excitation-dependent, effective nonlinear refractive index with previous observations of self-mode-locking in VECSELS. In Ref. 14, self-mode-locking in a V-cavity was shown to possibly originate from a negative nonlinear refractive index on the order of  $10^{-16} \text{ m}^2/\text{W}$ . Interestingly, when increasing the pump power, the measured pulse width decreased from  $> 1$  ps to  $< 500$  fs, which probably guarantees a negative effective nonlinear refractive index over the whole excitation range as shown by our investigations.

In Ref. 40, self-mode-locking was reported for a linear cavity. The insertion of a slit in front of the outcoupling mirror allows only assuming Kerr-lens mode-locking with a nonlinear lens of the positive focal length. As the pulse length obtained in this experiment was 3.5 ps, a positive Kerr lens is indeed expected, and thus, the assumption of Kerr-lens mode-locking caused by a nonlinear refractive index in the order of  $10^{-16} \text{ cm}^2/\text{W}$  is justified.

Beyond assessing the feasibility of Kerr-lens mode-locking of VECSELS, transient nonlinear refractive index changes generally play a crucial role in modeling pulse formation of VECSELS as it causes chirped pulses. In the semi-classical approach used in Refs. 25 and 26 to model SESAM-mode-locking of VECSELS, the refractive index change induced by the changes in carrier occupation is modeled by the so-called linewidth-enhancement factor  $\alpha$  that relates transient pulse phase changes  $\Delta\varphi(t)$  to the time-dependent gain  $g(t)$ <sup>25</sup>

$$\Delta\varphi(t) = -\alpha g(t)/2. \quad (4)$$

However, our measurements show that the refractive index dynamics, which directly translates to the pulse phase changes via  $\Delta\varphi(t) = k\Delta n(t)$ , with  $k$  being the wave vector, differs significantly in shape and relative contributions of components with different time scales from the gain dynamics. Therefore, it appears useful to incorporate the response function of the refractive index measured here into pulse simulations for more realistic modeling instead of using the phenomenological parameter  $\alpha$ .

In conclusion, we have probed both the gain and refractive index dynamics of a VECSEL chip under conditions similar to laser operation. Our results allow us to retrieve the response function of the refractive index change and to predict a pulse-length dependent effective nonlinear refractive index, which is negative and in the order of  $10^{-16} \text{ m}^2/\text{W}$  for sub-ps pulse lengths but becomes positive for large excitation fluences and ps pulse lengths. These findings support the assumption of Kerr-lens mode-locking for some self-mode-locking

results obtained with VECSELS. Additionally, our results might improve modeling of pulse formation in VECSELS by providing the time-resolved refractive index response of a VECSEL in the gain regime that could be directly incorporated into pulse-shaping simulations instead of a constant linewidth-enhancement factor.

See the [supplementary material](#) for further information about the VECSEL characterization and additional beam deflection as well as Z-scan measurements.

The authors thank U. Höfer for providing the 200 kHz laser system. C.K. thanks all members of the Nonlinear Optics group at CREOL for outstanding support and useful discussions during his visit and acknowledges financial support by the Deutscher Akademischer Austauschdienst (DAAD). G.M. and T.B. gratefully acknowledge funding by the Deutsche Forschungsgemeinschaft (DFG) via Project-ID 223848855-SFB 1083 and GRK 1782. This work was funded by the DFG through project Grant Nos. DFG RA 2841/1-1 and DFG RA 2841/1-3. This work was performed, in part, at the Center for Integrated Nanotechnologies, an Office of Science User Facility operated for the U.S. Department of Energy (DOE) Office of Science by Los Alamos National Laboratory (Contract No. 89233218CNA000001) and Sandia National Laboratories (Contract No. DE-NA-0003525).

## AUTHOR DECLARATIONS

### Conflict of Interest

The authors declare no conflict of interest.

### DATA AVAILABILITY

The data that support the findings of this study are available from the corresponding author upon reasonable request.

## REFERENCES

- S. M. Link, D. J. H. C. Maas, D. Waldburger, and U. Keller, "Dual-comb spectroscopy of water vapor with a free-running semiconductor disk laser," *Science* **356**, 1164–1168 (2017).
- F. F. Voigt, F. Emaury, P. Bethge, D. Waldburger, S. M. Link, S. Carta, A. van der Bourg, F. Helmchen, and U. Keller, "Multiphoton in vivo imaging with a femtosecond semiconductor disk laser," *Biomed. Opt. Express* **8**, 3213–3231 (2017).
- R. Bek, S. Baumgärtner, F. Sauter, H. Kahle, T. Schwarzbäck, M. Jetter, and P. Michler, "Intra-cavity frequency-doubled mode-locked semiconductor disk laser at 325 nm," *Opt. Express* **23**, 19947–19953 (2015).
- M. Kuznetsov, F. Hakimi, R. Sprague, and A. Mooradian, "High-power (>0.5-W CW) diode-pumped vertical-external-cavity surface-emitting semiconductor lasers with circular TEM<sub>00</sub> beams," *IEEE Photonics Technol. Lett.* **9**, 1063–1065 (1997).
- A. Rahimi-Iman, "Recent advances in VECSELS," *J. Opt.* **18**, 093003 (2016).
- M. Guina, A. Rantamäki, and A. Härkönen, "Optically pumped VECSELS: Review of technology and progress," *J. Phys. D: Appl. Phys.* **50**, 383001 (2017).
- F. Zhang, B. Heinen, M. Wichmann, C. Möller, B. Kunert, A. Rahimi-Iman, W. Stolz, and M. Koch, "A 23-watt single-frequency vertical-external-cavity surface-emitting laser," *Opt. Express* **22**, 12817–12822 (2014).
- M. Scheller, J. M. Yarbrough, J. V. Moloney, M. Fallahi, M. Koch, and S. W. Koch, "Room temperature continuous wave milliwatt terahertz source," *Opt. Express* **18**, 27112–27117 (2010).
- D. Waldburger, S. M. Link, M. Mangold, C. G. E. Alfieri, E. Gini, M. Golling, B. W. Tilma, and U. Keller, "High-power 100 fs semiconductor disk lasers," *Optica* **3**, 844–852 (2016).
- A. Laurain, I. Kilen, J. Hader, A. R. Perez, P. Ludewig, W. Stolz, G. Balakrishnan, S. W. Koch, and J. V. Moloney, "Modeling and experimental realization of modelocked VECSEL producing high power sub-100 fs pulses," *Appl. Phys. Lett.* **113**, 121113 (2018).
- K. G. Wilcox, A. C. Tropper, H. E. Beere, D. A. Ritchie, B. Heinen, and W. Stolz, "4.35 kw peak power femtosecond pulse mode-locked VECSEL for super-continuum generation," *Opt. Express* **21**, 1599–1605 (2013).
- Y. F. Chen, Y. C. Lee, H. C. Liang, K. Y. Lin, K. W. Su, and K. F. Huang, "Femtosecond high-power spontaneous mode-locked operation in vertical-external cavity surface-emitting laser with gigahertz oscillation," *Opt. Lett.* **36**, 4581–4583 (2011).
- L. Kornaszewski, G. Maker, G. P. Malcolm, M. Butkus, E. Rafailov, and C. J. Hamilton, "SESAM-free mode-locked semiconductor disk laser," *Laser Photonics Rev.* **6**, 20–23 (2012).
- A. R. Albrecht, Y. Wang, M. Ghasemkhani, D. V. Seletskiy, J. G. Cederberg, and M. Sheik-Bahae, "Exploring ultrafast negative Kerr effect for mode-locking vertical external-cavity surface-emitting lasers," *Opt. Express* **21**, 28801–28808 (2013).
- M. Gaafar, P. Richter, H. Keskin, C. Möller, M. Wichmann, W. Stolz, A. Rahimi-Iman, and M. Koch, "Self-mode-locking semiconductor disk laser," *Opt. Express* **22**, 28390–28399 (2014).
- R. Bek, M. Großmann, H. Kahle, M. Koch, A. Rahimi-Iman, M. Jetter, and P. Michler, "Self-mode-locked AlGaInP-VECSEL," *Appl. Phys. Lett.* **111**, 182105 (2017).
- K. G. Wilcox and A. C. Tropper, "Comment on SESAM-free mode-locked semiconductor disk laser," *Laser Photonics Rev.* **7**, 422–423 (2013).
- M. A. Gaafar, A. Rahimi-Iman, K. A. Fedorova, W. Stolz, E. U. Rafailov, and M. Koch, "Mode-locked semiconductor disk lasers," *Adv. Opt. Photonics* **8**, 370–400 (2016).
- E. Escoto and G. Steinmeyer, "Pseudo mode-locking," in *Proceedings of SPIE, Vertical External Cavity Surface Emitting Lasers (VECSELS) X* (SPIE, 2020), Vol. 11263, pp. 1–3.
- A. H. Quarterman, M. A. Tyrk, and K. G. Wilcox, "Z-scan measurements of the nonlinear refractive index of a pumped semiconductor disk laser gain medium," *Appl. Phys. Lett.* **106**, 011105 (2015).
- E. A. Shaw, A. H. Quarterman, A. P. Turnbull, T. Chen Sverre, C. R. Head, A. C. Tropper, and K. G. Wilcox, "Nonlinear lensing in an unpumped antiresonant semiconductor disk laser gain structure," *IEEE Photonics Technol. Lett.* **28**, 1395–1398 (2016).
- A. H. Quarterman, S. Mirkhanov, C. J. Smyth, and K. G. Wilcox, "Measurements of nonlinear lensing in a semiconductor disk laser gain sample under optical pumping and using a resonant femtosecond probe laser," *Appl. Phys. Lett.* **109**, 121113 (2016).
- C. Kriso, S. Kress, T. Munshi, M. Großmann, R. Bek, M. Jetter, P. Michler, W. Stolz, M. Koch, and A. Rahimi-Iman, "Microcavity-enhanced Kerr nonlinearity in a vertical-external-cavity surface-emitting laser," *Opt. Express* **27**, 11914–11929 (2019).
- C. Kriso, S. Kress, T. Munshi, M. Grossmann, R. Bek, M. Jetter, P. Michler, W. Stolz, M. Koch, and A. Rahimi-Iman, "Wavelength and pump-power dependent nonlinear refraction and absorption in a semiconductor disk laser," *IEEE Photonics Technol. Lett.* **32**, 85–88 (2020).
- R. Paschotta, R. Häring, A. Garnache, S. Hoogland, A. C. Tropper, and U. Keller, "Soliton-like pulse-shaping mechanism in passively mode-locked surface-emitting semiconductor lasers," *Appl. Phys. B: Lasers Opt.* **75**, 445–451 (2002).
- O. D. Sieber, M. Hoffmann, V. J. Wittwer, M. Mangold, M. Golling, B. W. Tilma, T. Südmeyer, and U. Keller, "Experimentally verified pulse formation model for high-power femtosecond VECSELS," *Appl. Phys. B: Lasers Opt.* **113**, 133–145 (2013).
- M. R. Ferdinandus, H. Hu, M. Reichert, Z. Wang, D. J. Hagan, and E. W. Stryland, "Beam deflection measurement of time and polarization resolved nonlinear refraction," *Opt. Lett.* **38**, 3518–3521 (2013).
- M. Sheik-Bahae, A. A. Said, T. H. Wei, D. J. Hagan, and E. W. Van Stryland, "Sensitive measurement of optical nonlinearities using a single beam," *IEEE J. Quantum Electron.* **26**, 760–769 (1990).
- Z. Yang, A. R. Albrecht, J. G. Cederberg, and M. Sheik-Bahae, "Optically pumped DBR-free semiconductor disk lasers," *Opt. Express* **23**, 33164 (2015).

- <sup>30</sup>H. Kahle, C. M. N. Mateo, U. Brauch, P. Tatar-Mathes, R. Bek, M. Jetter, T. Graf, and P. Michler, "Semiconductor membrane external-cavity surface-emitting laser (MECSEL)," *Optica* **3**, 1506–1512 (2016).
- <sup>31</sup>Z. Yang, D. Follman, A. R. Albrecht, P. Heu, N. Giannini, G. D. Cole, and M. Sheik-Bahae, "16 W DBR-free membrane semiconductor disk laser with dual-SiC heatspreader," *Electron. Lett.* **54**, 430–432 (2018).
- <sup>32</sup>K. Hall, J. Mark, E. Ippen, and G. Eisenstein, "Femtosecond gain dynamics in InGaAsP optical amplifiers," *Appl. Phys. Lett.* **56**, 1740–1742 (1990).
- <sup>33</sup>A. Othonos, "Probing ultrafast carrier and phonon dynamics in semiconductors," *J. Appl. Phys.* **83**, 1789–1830 (1998).
- <sup>34</sup>J. Mork and A. Mecozzi, "Response function for gain and refractive index dynamics in active semiconductor waveguides," *Appl. Phys. Lett.* **65**, 1736–1738 (1994).
- <sup>35</sup>C. G. E. Alfieri, D. Waldburger, S. M. Link, E. Gini, M. Golling, G. Eisenstein, and U. Keller, "Optical efficiency and gain dynamics of modelocked semiconductor disk lasers," *Opt. Express* **25**, 6402 (2017).
- <sup>36</sup>C. Baker, M. Scheller, S. W. Koch, A. R. Perez, W. Stolz, R. J. Jones, and J. V. Moloney, "In situ probing of mode-locked vertical-external-cavity-surface-emitting lasers," *Opt. Lett.* **40**, 5459–5462 (2015).
- <sup>37</sup>J. Mork, A. Mecozzi, and C. Hultgren, "Spectral effects in short pulse pump-probe measurements," *Appl. Phys. Lett.* **68**, 449–451 (1996).
- <sup>38</sup>M. Reichert, H. Honghua, M. R. Ferdinandus, M. Seidel, P. Zhao, T. R. Ensley, D. Peceli, J. M. Reed, D. A. Fishman, S. Webster, D. J. Hagan, and E. W. Van Stryland, "Temporal, spectral, and polarization dependence of the nonlinear optical response of carbon disulfide," *Optica* **1**, 436–445 (2014).
- <sup>39</sup>M. Sheik-Bahae and E. Van Stryland, "Ultrafast nonlinearities in semiconductor laser amplifiers," *Phys. Rev. B* **50**, 14171–14178 (1994).
- <sup>40</sup>A. Rahimi-Iman, M. Gaafar, C. Möller, M. Vaupel, F. Zhang, D. Al-nakdali, K. A. Fedorova, W. Stolz, E. U. Rafailov, and M. Koch, "Self-mode-locked vertical-external-cavity surface-emitting laser," in *Proceedings of SPIE, Vertical External Cavity Surface Emitting Lasers (VECSELs) VI* (SPIE, 2016), Vol. 9734, p. 97340M.